Rapid Prototyping J

Computer-aided methods for single stage fibrous dysplasia excision and reconstruction in the zygomatico-orbital complex

Journal:	*Rapid Prototyping Journal*
Manuscript ID	RPJ-05-2018-0116.R2
Manuscript Type:	Original Article
Keywords:	Computer aided modelling, Additive Manufacturing (AM), Patient-specific implant, Surgical guides, Design

Computer-aided methods for single stage fibrous dysplasia excision and reconstruction in the zygomatico-orbital complex

***Abstract*:**

Purpose - Computer Aided Design and Additive Manufacture (CAD/AM) technologies are sufficiently refined and meet the necessary regulatory requirements for routine incorporation into the medical field, with long-standing application in surgeries of the maxillofacial and craniofacial region. They have resulted in better medical care for patients, and faster, more accurate procedures. Despite ever-growing evidence about the advantages of computer aided planning, CAD and AM in surgery, detailed reporting on critical design decisions that enable methodological replication, and the development and establishment of guidelines to ensure safety, are limited.

Design/methodology/approach - This paper presents a novel application of CAD and AM to a single stage resection and reconstruction of fibrous dysplasia in the zygoma and orbit. It is reported in sufficient fidelity to permit methods replication and design guideline developments in future cases, wherever they occur in the world. The collaborative approach included engineers, designers, surgeons and prosthetists to design patient-specific cutting guides and a custom implant. An iterative design process was used, until the desired shape and function were achieved, for both of the devices. The surgery followed the CAD plan precisely and without problems. Immediate post-operative subjective clinical judgements were of an excellent result.

Findings - At 19 months post-op, a CT scan was undertaken to verify the clinical and technical outcomes. Dimensional analysis showed maximum deviation of 4.73 mm from the plan to the result, while CAD-Inspection showed that the deviations range between -0.1 and -0.8 mm, and that the majority of deviations are located around the –0.3 mm.

Originality/value - Improvements are suggested and conclusions drawn regarding the design decisions considered critical to a successful outcome for this type of procedure in the future.

Keywords: CAD modelling, Additive manufacturing (AM), patient-specific implant, surgical guides, design

Paper type Case study

1. INTRODUCTION

The application of medical imaging, Computer Aided Design (CAD), Computer Aided Manufacture (CAM), and Additive Manufacturing (AM) in medicine is evolving at a rapid pace. In early years of development, these technologies were largely the preserve of the aerospace, automotive and other engineering sectors. Early reported clinical applications emerged in the 1990s (Mankovich, et al, 1990), driven by advances in medical imaging, particularly Computed Tomography (CT), used in combination with software developed to translate the Hounsfield values of tissue types into three-dimensional (3D) models (Swaelens & Kruth, 1993). CAD/CAM/AM were enthusiastically adopted in head and neck reconstruction, most likely due to the complex anatomical structures that are difficult to visualize. Reconstruction of the craniofacial skeleton still represents a major challenge even for the most experienced surgeons when using the most advanced technologies. Some of the key factors contributing to complexity of those procedures include the presence of vital anatomy in the close vicinity of the treated region, uniqueness of every clinical case, as well as the chances for potential infection (Parthasarathy, 2014). What's more, the fidelity of clinical case reports in the literature is often lacking sufficient fidelity to permit criticism of employed techniques, and to enable subsequent evidence-based refinement (Burton et al, 2018). Widely accepted specific design guidelines do not exist for this reason, and for reasons of commercial secrecy, limited follow-up, inconsistent outcome measures, and a lack of joint clinician-designer perspectives. Some initial work has been undertaken for complex craniofacial reconstructions (Peel et al, 2017).

This paper focuses on a single complex surgical case study. This is common in the field; due to the ethical barriers from directly comparing CAD and AM methods to conventional equivalents predicted to be inferior on an individual patient basis. The way in which these technologies are applied has changed significantly since the early years of development; it has evolved from fabricating replica models of patient anatomy in polymer (Almoatazbellah et al, 2017), to the use of 3D computer aided planning, device design and AM production of the final use devices (Salmi, 2016). There is indeed increasing published evidence that customized implants, used in combination with guides, offer advantages compared to off-the-shelf alternatives. Research illustrates that using CAD/AM can: offer a more accurate fit reduce theatre time, and reduce the likelihood of needing surgical revisions (Singare et al, 2009, Peel et al, 2017); decrease stress shielding and the likelihood of bone resorption (Harrysson et al 2008); incorporate tailored mechanical properties (Parthasarathy et al, 2011); and improve osseointegration (Palmquist et al, 2011). Publications demonstrate this in, as examples, implant types ranging from cranioplasty plates (Poukens et al, 2008), to orbital floor implants (Salmi et al, 2012), and complex osteotomies (Peel et al, 2016a). Improving the predictability of complex procedures is perhaps one of the greatest advantages afforded by a CAD/AM approach. And with the increasing research performed in the use of AM technologies for their application in biomaterials and (re)generation of tissues and organs (Zadpoor et al, 2017), the future of these technologies is looking bright and prosperous.

2. MATERIALS AND METHODS

2.1. The patient

The 25 year old male patient, had undergone an initial surgical procedure at the age of 18 to correct facial asymmetry for aesthetic purposes. This represented conservative initial treatment of fibrous dysplasia (FD). Surgical access was through upper jaw fornix. Bone levelling was performed, while the histopathological report confirmed fibro osseous dysplasia. After seven years, the patient returned with a deformity which was even more prominent than before the first surgery. Given the advanced stage of the patient's condition and complexity of the

proposed corrective surgery, the surgical team decided that guided bone excision and a restorative custom implant would be the most effective and safe option.

The goal was to achieve satisfactory aesthetic results, whilst preserving the patient's vision through minimal surgical site exposure and face scarring, by completely removing zygomatic bone and replacing it with the implant.

Signed consent has been previously obtained from the patient for publication of research results presented in this paper.

2.2. Approach

The patient was scanned on a Multi-slice CT (MS CT), Siemens 64, with the 512x512 resolution and slice thickness of 0.70 mm. The output was in the form of DICOM files (Digital Imaging and Communications in Medicine). Specialist software (Mimics V18, Materialise, Belgium) was used to generate 3D surface models of the patient's anatomy based on the Hounsfield unit range of bone (298-3071) using reported techniques (Thomas et al, 2017). Semi-automated segmentation of the lesion was also undertaken with the boundaries defined by the surgeon. Upon completion, the 3D models of the normal bony structure and lesion were exported as STereoLithography (STL) files using high quality settings for fabrication using an AM machine (Z310 Plus, Z-Corporation - 3D Systems) with a view to improving early-stage visualization. The Z-Corp machine was used due to its availability, and because of the high speed and low material costs. It had been calibrated for accuracy by the operators. Standard ceramic powder, ZP131 was used, with a layer thickness of 0.1 mm. After printing, the model was infiltrated to achieve its final mechanical properties. For this purpose, cyanoacrylate was used. Once infiltrated and dried, the model of the isolated disease (Fig. 1) was ready for detailed analysis and planning of the surgical procedure.

Figure 1. a) Preoperative CT image of the patient, b) Anatomical model of the face with lesion produced using AM

2.3. Planning of surgical procedure

Computer aided planning was chosen as a method to rehearse the procedure whilst minimizing the need for multiple physical models. The STL geometry of the skull anatomy and lesion were imported into FreeForm Modeling Plus version 2016 (3D Systems, Rock Hill, USA), which has been widely reported for implant design (Peel et al, 2017). FreeForm was operated by a dedicated design engineer with experience in implant and guide design. Clinical direction was provided by the prescribing maxillofacial surgeon; who had discussed the possibilities with other members of the surgical team. The first step was Boolean subtraction of the FD-affected bone from the healthy anatomy (Fig. 2b).

Figure 2. Image of 3D model with a) disease boundaries, and b) after subtraction

2.4. Design process

The surgeon provided essential design criteria through initial consultations with the design engineer. This included the instruction to ensure simplicity of the design solution and consider the potential for the FD margin to have changed slightly between the CT scan and date of surgery. The design process was also performed in FreeForm. Mirror based reconstruction was used as the basis of modelling the missing region. A portion of the patient's healthy, right side was mirrored across the mid sagittal plane and copied to the left side. The patient's anatomy was protected from accidental modification using the 'Buck' setting in FreeForm. The mirrored portion of midface anatomy was then sculpted to more closely blend into the surrounding anatomy using tools in the 'Sculpt Clay' palette. The 'Clay' was then joined to the 'Buck' anatomy model and blended using the 'Hot Wax' tools to create a smooth, symmetry-based reconstruction (Fig 3).

Figure 3. Designing of missing region using mirror-based reconstruction approach

With primary reconstruction completed, the location of screw holes were considered based upon the bone quality and need to avoid sensitive anatomical structures. CAD versions of the intended 1.5mm diameter screws were imported as 'Mesh' structures. 'Mesh' structures protect the sharp edge detail of STL files imported into FreeForm. Axis markers were positioned perpendicular to the bone surface in the desired locations for the screws: the supraorbital rim, zygomatic arch and medially on the infraorbital rim. This intended to maximise screw thread-bone engagement. The screws were aligned to the axis markers and placed at the intended depth into the bone. These initial positions were confirmed as suitable by exporting the screws as STL files and importing them into the Mimics file to accurately assess bone quality and relationships to sensitive anatomy, particularly in the medial infraorbital rim area.

A duplicate of the 'Buck' anatomy with combined reconstruction was then made. The 'Buck' anatomy was then removed leaving just the reconstruction. The 'Clay' coarseness was reduced, which had a smoothing effect. The main body of the 'Clay' shape was selected, the selection was inverted and any unattached pieces of 'Clay' were removed, which left a draft form of the implant shape. This shape was duplicated to ensure a reference was available for future modifications. One version of the implant shape was then shelled to a thickness of 1mm. The posterior/deep portions in the maxilla region were manually carved away, leaving an outer shell in that area, and hollow structure along the zygomatic arch with open ends (Fig. 4). This was based on the surgeon's instruction to reduce the bulk of alloplastic material. Edges that interfaced with the bone were reduced to provide a gap that would account for FD margin change. This was based on design guidelines reported in literature (Peel et al, 2017).

Figure 4. a) The outer (superficial) side of the hollow implant, b) the inside (deep) side of the implant

A document describing the design was presented to the prescribing surgeon for review. The surgeon specified modifications: reduce the size of the orbital floor area, add holes in the infraorbital rim area and slightly reposition the location of the screws in the supraorbital rim. These changes were carried out and an updated document was provided to the surgeon. These modifications were requested by the surgeon as it was easier to visualize the final shape of the implant after seeing an initial design. Once the design details were confirmed and the screw positions were finalized, tabs that extended from the 'Clay' reconstruction were designed to overlap on to the surface of the anatomy. These were joined and blended into to the main body of the implant. The implant design was converted to a 'Mesh' structure and the CAD screws were Boolean subtracted. Final design checks were made and Boolean operations of the anatomy from the implant were undertaken to ensure there was no interference between it and the bone. Figure 5 shows the completed implant design.

Figure 5. The completed implant design

In order to accurately pre-drill holes for the fixation screws and ensure the tumour was removed according to the computer plan, the surgeon prescribed drilling/cutting guides (one for the supraorbital rim and one for the zygomatic arch). Pre-designed tubes with a triangular cross section designed to accept a 1.25mm diameter pilot drill were imported as 'Mesh structures and positioned in the same axis as each screw where pre-drilling was desired. Triangle profile sections were used to reduce the chances of the drill binding and promote irrigation of the cutting site, whilst ensuring the desired vector was followed through three-point contact. Cutting planes and surface patches that indicated the vector for saw cuts were then created. The surface patches were converted to a

clay thickness. 1mm thickness of 'Clay' was added to the protected 'Buck' anatomy around the side of the anatomy to remain after the cuts. Care was taken to ensure these surfaces engaged contours that would provide a secure location during the drilling/cutting process. Various modelling tools were used to join cutting surfaces and bone interfacing surfaces before converting the design to a 'Mesh' structure. The tube sections were then Boolean added to the guide bodies and final checks as described in the implant design process were undertaken. Figure 6 shows the completed guides.

Figure 6. The surgical guides for disease removal

2.5. Analysis of the implant design

Figure 7 shows the analysis of the overlap of the modelled implant with the removed pathology. This analysis helped the surgeon to understand how much bulk would be removed and consider the aesthetic impact. Recording this detail was also considered important to inform future cases.

Figure 7. Analysis of the overlap of the modelled implant with the removed disease

Five control points were defined on the FD mass and the implant, which provided the basis for calculation of the distance between them (Fig. 8).

Figure 8. Distance between disease and implant at five control points

Figure 8 shows that the largest distance between the diseased original bone and planned implant location was 23.59 mm, and was located in the lower region, where the FD had spread the most. In the frontal plane, the difference in thickness was 6.74 mm, 5.62 mm and 7.65 mm. In the orbital section, the difference in thickness was 7.21 mm. The analysis allowed the conclusion that the FD removal and its replacement by a titanium implant represented an appropriate choice.

2.6. Device Fabrication

The final implant and guide designs were exported as STL files with accompanying manufacturing instructions. A smooth, satin outer finish (0.725 um +/- 0.007 um) was specified for the implant on the basis that it would prevent soft tissue adhesion and reduce the level of light reflected back through the soft tissue (potentially making it less visible). The guides were specified with an as-manufactured, rough surface finish to ensure they had higher friction against the bone when in use for improved grip. Documentation that described the devices and illustrated how they interfaced with the anatomy was also provided to the prescribing surgeon. The device STL files were transferred for fabrication in an ISO13485 accredited manufacturing facility (Renishaw PLC, Miskin, UK). Production engineers supported the implant and guides for fabrication using QuantAM file preparation software (Renishaw PLC, UK). The implants were fabricated by Laser Melting (LM) (AM250, Renishaw, Miskin, UK) using Ti6Al-4V ELI (grade 23). The production engineers then followed standard medical implant post processing procedures including proprietary heat treatment cycle in a vacuum furnace to optimise part flexibility and mechanical properties. The outer (soft tissue facing) surface was finished using powered hand tools before being grit blasted using manufacturer proprietary methods. The inner surface was grit blasted only. The devices then underwent ultrasonic cleaning, drying and passivization before being packaged for dispatch. Figure 9 shows the completed implant outer and inside surfaces. Figure 10 shows the two guides.

Figure 9. Implant fabricated from Titanium alloy

Figure 10. The guides with 1.25 mm openings which allow fixation during bone excision

2.7. Surgical procedure

Standard, manufacturer specified methods of autoclave sterilization were used prior to surgery. Sterilization parameters are given in Table 1.

Table 1 Sterilization parameters of Autoclave system

The localization of osteophobic change was only on the zygomatic area with slight involvement of the maxilla and frontal bone, which required an open access cut by Weber in order to make a complete resection. The surgical intervention itself went without any unplanned events. The cut was made at places planned by placing the resection guides, as shown on figure 11. The implant was fixed with the 1.5mm diameter titanium screws.

Figure 11. Image a) and b) showing surgical procedure on the patient, and c) the condition after the procedure

3. RESULTS

Once the surgical procedure was successfully completed, the patient was given time to recuperate. After the usual post-operative swelling reduced, the significantly improved aesthetic and facial symmetry of the patient were visible.

After the first day, radiographic imaging was performed in order to confirm the implant location and visualise the relationship of the boy anatomy and implant (Figure 12). The patient was hospitalized for 7 days, and antibiotic prophylaxis was carried out. The sutures were removed 10 days after the operative procedure.

Figure 12. Condition before and after the surgical procedure

One year and seven months after the surgery, a post-operative CT scan was performed in order to examine the current situation on the progress (Figure 13). Patient was scanned again using the same protocols as previously described.

The long-standing nature of the pre-operative bone growth had acted as an expander and thus reduced the thickness of soft tissue, which, post-operatively manifested as a mild asymmetry of the face. The patient also reduced his body weight by 10 kilos for a year, due to intense sports training.

Figure 13. Post-operative check-up

In order to quantify the success of surgery, the STL file of the pre-operative plan was aligned with the 3D model of the post-operative scan. The software used for alignment was GOM Inspect v2018 (GOM GmbH, Braunschweig, Germany). The “Prealignment” tool was used for initial alignment of two 3D models which was followed by “Local Best-fit” method used for accurate alignment of the pre-operative plan and post-operative scan STL files of implant in order to access the current state. Afterwards, 3D model of the pre-operative plan was imported and overlaid on top of the DICOM images of the post-operative scan in Mimics Research V18 (Materialise, Leuven, Belgium) software in order to perform necessary measurements.

Figure 14. Post-operative scan with measurements on a) axial view, b) coronal view, c) sagittal view and d) the locations on where the measurements have been taken

The post-operative scan shows some deviations compared to the pre-operative plan. Figure 14 shows the areas where the deviations are the largest from the pre-operative plan (yellow) for the zygomatico-orbital implant and bone (white) in the axial, coronal and sagittal planes.

The deviation of 2.81 mm, shown on figure 14a, is located in the axial view, and it is located in the upper area of the implant near the place where the implant is fixed to the bone with screws. In the figure 14b (taken from a 2D slice from the zygomatic bone towards the zygomatic process) it can be seen that the deviation in this area is 1.98 mm, when examined from the coronal view. Also from figure 14c, in the sagittal view, the maximum deviations were noticed on the zygomatic process area and they are 4.73 mm, while some movement during fixation of the screw above eyebrow shows deviation of 3.21 mm.

Also, CAD-Inspection analysis was performed in order to examine the overall position of the post-operative scan compared to the pre-operative plan where the green colour is indicating that deviations are within pre-defined limits, blue colour is indicating that the surface of the post-operative scan is pushed deeper than the surface of the pre-operative plan and the red colour is indicating that the surface of the post-operative scan is located above the surface of the pre-operative plan (Figure 15). The software used for this was also GOM Inspect v2018.

Figure 15. CAD-Inspection analysis of 3D models from pre-operative plan and the post-operative scan

From CAD-Inspection it can be noticed that the majority of deviations are between -0.1 mm and -0.8 mm, while the peak of deviations concentration is around the –0.3 mm mark. The overall deviation inspection shows some movement of the implant towards the zygomatic process. However, the implant retained its overall position and analysis demonstrated that the surgical procedure was a success.

4. DISCUSSION

These results must be considered in the context of the study limitations, prior to evaluating their relevance. This was a single clinical case study of a rare, but complex procedure. This makes it difficult to compare with previous reported cases or draw conclusions that could be considered statistically significant. Notwithstanding this limitation, this case study provides the opportunity to report important design and manufacturing considerations that can be used to inform future research or application of these methods in similar cases.

4.1. Cross-discipline working

Previous research has identified the value of cross-discipline working (Truscott et al, 2007) to achieve a successful outcome when using CAD/AM techniques. This case required the application of complex computer aided planning/design software with a detailed understanding of design process and the manufacturing process. This needed to be combined with knowledge of the clinical condition and surgical techniques. At the time of writing, it is rare to have each of these complex skills available within a hospital environment. The importance of creating a high fidelity specification for design and manufacture therefore becomes critical to ensure patient safety and reduce the number of design iterations required to create the final device (Peel et al, 2016b). Relatively simple communication and design validation tools were used in this case to ensure that the prescribing surgeon was satisfied with the implant and guide designs. This included the use of clear illustrated images that described the devices and their critical interfaces with the anatomy. Other communication methods include embedding interactive 3D models within Portable Document Files (.PDF) and over-the-internet 3D CAD file sharing. These methods enable collaborative working without being constrained to specific time slots for screen shares. Given the importance of collaborative working in cases like this, the effectiveness of specific communication tools should be investigated further. As in-hospital skills sets evolve, the trend for regionalized centers of healthcare design and engineering continues to develop and CAD software becomes more

automated, current cross-discipline communication challenges may be overcome.

4.2. Design details

Material selection was the first critical decision. The surgeon could have chosen two reconstruction methods: alloplastic materials or autogenous tissue. Autogenous tissue was discounted due to the fact it would have required harvesting vascularized tissue from another area of the body, increasing infection risk and surgery duration. There were two well-documented alloplastic materials choices: titanium and Polyether ether ketone (PEEK). Titanium was chosen due to its long history of acceptance for deep buried implant use, lower relative cost and ability to be fabricated using AM. AM allowed the design to incorporate fixation tabs, thin wall sections and other features that would have been difficult to fabricate with alternative computer-based manufacturing methods. Screws were placed away from sensitive anatomy and sufficiently clear of the implant/bone margin. They were also countersunk into the implant to avoid the potential for overlaying soft tissue irritation. A smooth satin surface finish was chosen to reduce the potential for soft tissue adhesion and reflectance (which could potentially make the implant visible through thin overlaying tissue). The clinical evidence to support the surface finish decision was, however, relatively limited; titanium is well known for its ability to osseointegrate with bone, but there is less evidence describing how it reacts to overlaying soft tissue when used in cases like this (Cox et al, 2017). Implants produced using metal AM are inherently rough (in the order of 34 ± 8 to 22 ± 3 µm) and need extensive automated and manual finishing to achieve the grades of surface finish typically applied to medical implants. This adds time and cost to the production process. The clinical and aesthetic implications of surface finish on cranio-maxillofacial implants requires further investigation. The implant reported in this case was specified with a 1mm thickness with material bulk removed from the maxilla area. In general, it is best practice to reduce the amount of alloplastic material implanted and in the case of AM produced implants, this can also aid in reducing internal stresses during the build process. From an AM perspective, the implant in this case could have benefitted from the use of a lattice or highly perforated structure in order to further-reduce the potential for internal stress build up. However, published evidence that describes both the clinical implications of highly perforated implants and the implications on ease of AM is limited. This is another area where further investigations are required to conclude design guidelines.

Specific design and manufacturing guidelines can be extracted from this case: the need to consider whether the disease extent could have changed between the CT scan date to surgery date; extent of the orbital floor; material choice; screw locations; surface finish and; material bulk. Fibro osseous dysplasia is a relatively slow-changing condition, which meant that the extent of bony anatomy change was likely to be minimal between CT scan and surgery date. Nevertheless, the implant was designed to locate with a 1-2mm gap between the excised bone and metal and the fixation tabs were extended to ensure sufficient overlap should more of the bone have required removal. For fast-growing tumors, these design considerations become even more critical. The surgeon requested that the orbital floor portion on the implant was reduced. As it was not completely clear how much of orbital floor bone would be needed to be removed, the implant was shortened at that area while the orbital floor bone was reconstructed by polydioxanone (PDS) mesh during the operation.

The accuracy deviations observed and illustrated in figure 14 were likely the consequence of parameters such as:

- CT accuracy;
- small changes in anatomical structure during the time between imaging and operation;
- misalignments during the surgical procedure;
- anatomical changes during the healing process.

Further work is required to identify the potential impact of tolerance stacking throughout

the image acquisition through design, manufacture and surgery.

4.3. Infrastructure & regulatory considerations

Unlike implants produced from stock plating and mesh systems in hospital laboratories, commercially produced patient specific implants must conform to strict quality management and regulatory standards. With evolving regulatory requirements that require the adoption of quality management systems in hospital laboratories, it is possible to envisage a medium term future in which commercially produced patient-specific implants become the norm. Those responsible for designing, and using patient specific implants and guides must therefore place increasing importance on controlling the design process. Reporting specific design considerations, new rules or guidelines, manufacturing details and, where possible, correlating those to clinical outcomes is therefore crucial. It is also important for those reporting case studies and series to report negative outcomes, including where implants have failed. Without such detail, it will become difficult for surgeons to prescribe devices that are appropriate, designers to make informed decisions that harness the freedoms afforded by AM and manufacturers to refine parameters.

5. CONCLUSIONS

The use of a customized implant and guides allowed the surgeon to undertake the procedure with a greater degree of confidence. Specific design decisions that helped to ensure safety and efficiency are reported here, and should be reported in detail across the field to permit replication and development. These design guidelines should be considered in the context of advances in AM technology and materials, the need for effective cross-disciplinary working, and changing regulatory frameworks. It is clear that the hybrid of biology, design, and engineering is challenging the way medicine is practiced and is providing exciting new opportunities in the way disease, trauma, and congenital conditions are treated.

6. ACKNOWLEDGEMENTS

This paper presents the results achieved in the framework of the Project no. 114-451-2723 / 2016-03 funded by the Provincial Secretariat for Higher Education and Scientific Research, and within the project TR - 35020, funded by the Ministry of Education, Science and Technological Development of Republic of Serbia.

7. REFERENCES

1. Almoatazbellah, Y., Hollister J. S., and Dalton, P.D. (2017), “Additive manufacturing of polymer melts for implantable medical devices and scaffolds”, *Biofabrication,* Vol. 9 No. 1, pp. 1 – 29, DOI: https://doi.org/10.1088/1758-5090/aa5766
2. Burton, H. E., Peel, S. & Eggbeer, D. (2018), "Reporting fidelity in the literature for computer aided design and additive manufacture of implants and guides", *Additive Manufacturing,* 23(Oct) pp. 362-373 https://doi.org/10.1016/j.addma.2018.08.027
3. Cox S.C., Jamshidi P., Eisenstein N.M., Webber M.A., Burton H., Moakes R.J.A., Addison O., Attallah M., Shepherd D.E.T., and Grover L.M. (2017), “Surface Finish has a Critical Influence on Biofilm Formation and Mammalian Cell Attachment to Additively Manufactured Prosthetics”, *ACS Biomaterials Science & Engineering,* Vol. 3 No. 8, pp. 1616-1626, DOI: 10.1021/acsbiomaterials.7b00336
4. Harrysson, O., Cansizogly, O., Marcellin-Little, D.J., Cormier, D.R., & West Ii, H.A. (2008), "Direct metal fabrication of titanium implants with tailored materials and mechanical properties using electron beam melting technology", *Advanced Processing of Biomaterials Symposium, Materials Science and Technology Conference and Exhibition*. *Cincinnati, OH*, pp. 366-373.
5. Mankovich N.J., Cheeseman A.M., and Stoker N.G. (1990), "The Display of Three-dimensional Anatomy With Stereolithographic Models", *Journal of Digital Imaging,* Vol. 3 No. 3, pp. 200-203.

6. Palmquist, A., Snis, A., Emanuelsson, L., Browne, M. and Thomsen, P. (2011), "Long-term biocompatibility and osseointegration of electron beam melted, free-form–fabricated solid and porous titanium alloy: Experimental studies in sheep", *Journal of Biomaterials Applications*, Vol 27 No 8, pp. 1003-1016.
7. Parthasarathy, J., Starly, B. and Raman, S. (2011), "A design for the additive manufacture of functionally graded porous structures with tailored mechanical properties for biomedical applications", *Journal of Manufacturing Processes*, Vol. 13 No. 2, pp. 160-170.
8. Parthasarathy, J. (2014), "3D modeling, custom implants and its future perspectives in craniofacial surgery", *Annals of Maxillofacial Surgery*, Vol. 4 No.1, pp. 9–18.
9. Peel, S., Eggbeer, D., Sugar, A. and Evans, P. L. (2016a), "Post-traumatic zygomatic osteotomy and orbital floor reconstruction", *Rapid Prototyping Journal*, Vol. 22 No. 6, pp. 878–886.
10. Peel, S. and Eggbeer, D. (2016b), "Additively manufactured maxillofacial implants and guides – achieving routine use", *Rapid Prototyping Journal*, Vol. 22 No. 1, pp. 189–199.
11. Peel, S., Bhatia, S., Eggbeer, D., Morris, D., Hayhurst, C. (2017), "Evolution of design considerations in complex craniofacial reconstruction using patient-specific implants", *Proceedings of the Institution of Mechanical Engineers, Part H: Journal of Engineering in Medicine, Vol.* 231 No. 6, pp. 509–524.
12. Poukens, J., Laeven, P., Beerens, M., Nijenhuis, G., Sloten, J. V., Stoelinga, P., & Kessler, P. (2008), "A classification of cranial implants based on the degree of difficulty in computer design and manufacture", *The International Journal of Medical Robotics and Computer Assisted Surgery,* Vol. 4 No. 1, pp. 46-50.
13. Salmi, M., Tuomi, J., Paloheimo, K., Björkstrand, R., Paloheimo, M., Salo, J., Kontio, R., Mesimäki, K. and Mäkitie, A. (2012), "Patient-specific reconstruction with 3D modeling and DMLS additive manufacturing", *Rapid Prototyping Journal*, Vol. 18 No. 3, pp. 209-214.
14. Salmi, M. (2016), "Possibilities of preoperative medical models made by 3D printing or additive manufacturing" *Journal of Medical Engineering,* Vol. 2016, ID 6191526, pp. 1-6.
15. Singare, S., Lian, Q., Wang, W. P., Wang, J., Liu, Y., Li, D., & Lu, B. (2009), "Rapid prototyping assisted surgery planning and custom implant design", *Rapid Prototyping Journal,* Vol. 15 No. 1, pp. 19-23.
16. Swaelens B., Kruth J.P. (1993), "Medical applications of rapid prototyping techniques. In. *Proceedings of the 4th international conference of rapid prototyping*", pp. 107-117.
17. Thomas D., Jessop Z., Whitaker I. (2017), "Chapter - Computational Design of Biostructures", *3D Bioprinting for Reconstructive Surgery, 1st Edition*, Elsevier Publishing, London. Hardcover ISBN: 9780081011034.
18. Truscott, M., De Beer, D., Vicatos, G., Hosking, K., Barnard, L., Booysen, G. and Campbell, R.I. (2007), "Using RP to promote collaborative design of customised medical implants", *Rapid Prototyping Journal*, Vol. 13 No. 2, pp. 107-114.
19. Zadpoor, A. A., Malda, J. (2017), "Additive manufacturing of biomaterials, tissues, and organs", *Annals of Biomedical Engineering*, Vol. 45 No. 1, pp. 1-11.

UNIVERZITET U NOVOM SADU

MEDICINSKI FAKULTET

KLINIČKI CENTAR VOJVODINE

KLINIKA ZA MAKSILOFACIJALNU HIRURGIJU

SAGLASNOST

SAGLASAN SAM DA SE MOJE FOTOGRAFIJE I MEDICINSKI NALAZI KORISTE U NAUČNE SVRHE U OKVIRU ISTRAŽIVANJA NA KLINICI ZA MAKSILOFACIJALNU HIRURGIJU, KAO I DA SE MOJE FOTOGRAFIJE I NALAZI MOGU PREZENTOVATI U NAUČNIM RADOVIMA.

NOVI SAD 06.07.2018.

Prof. dr sci. med.
ALEKSANDAR KIRALJ
specijalista za maksilofacijalnu hirurgiju

SAGLASAN

MAKSIM ŠUŠNJAR

Table 1 Sterilization parameters of Autoclave system

Cycle temp.:	1340°C / 1210°C
Time:	3 minutes / 15 minutes
Porous load cycle:	Positive & negative pulsing
Drying time:	30 minutes

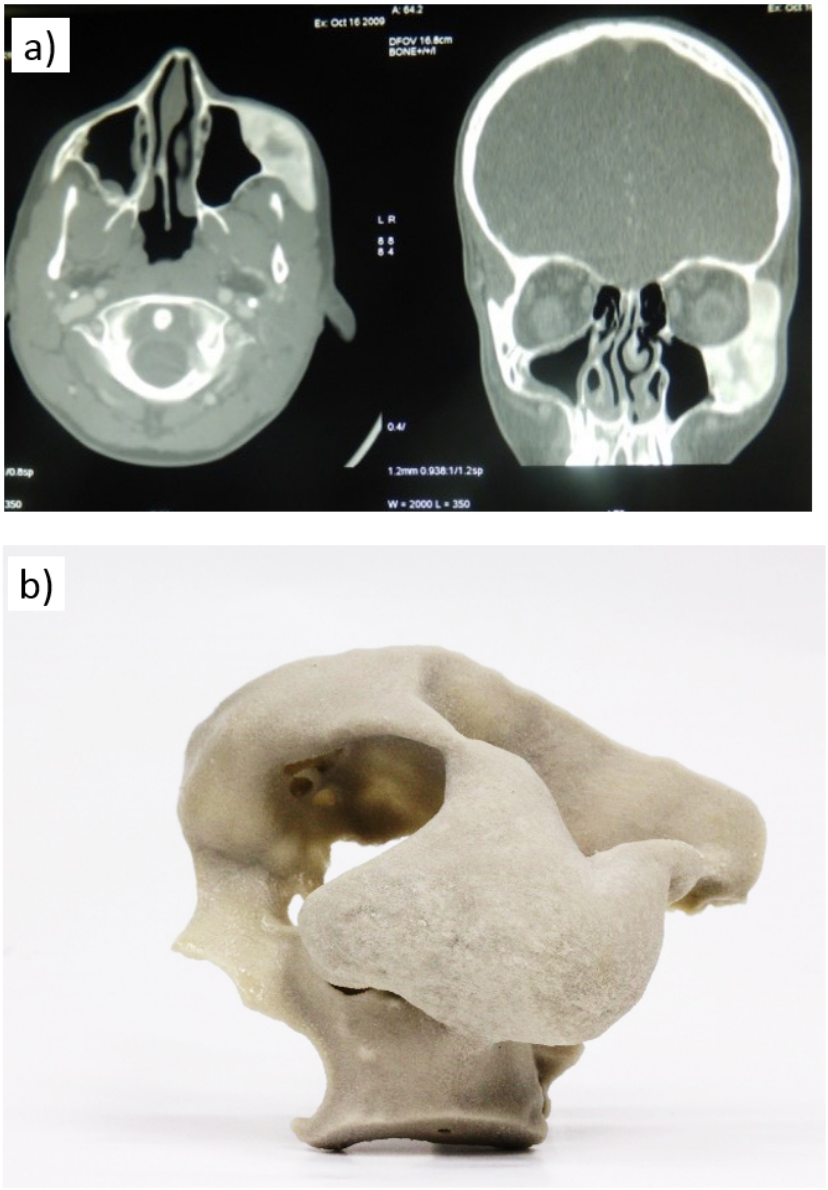

Figure 1. a) Preoperative CT image of the patient, b) Anatomical model of the face with lesion produced using AM

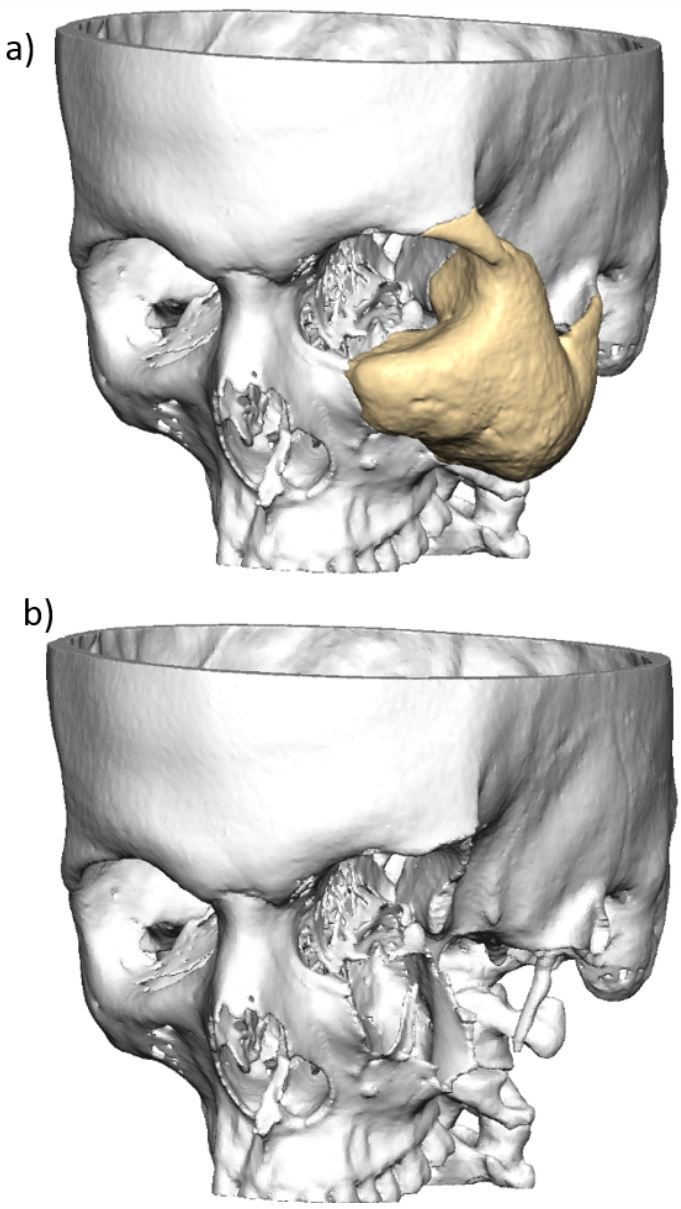

Figure 2. Image of 3D model with a) disease boundaries, and b) after subtraction

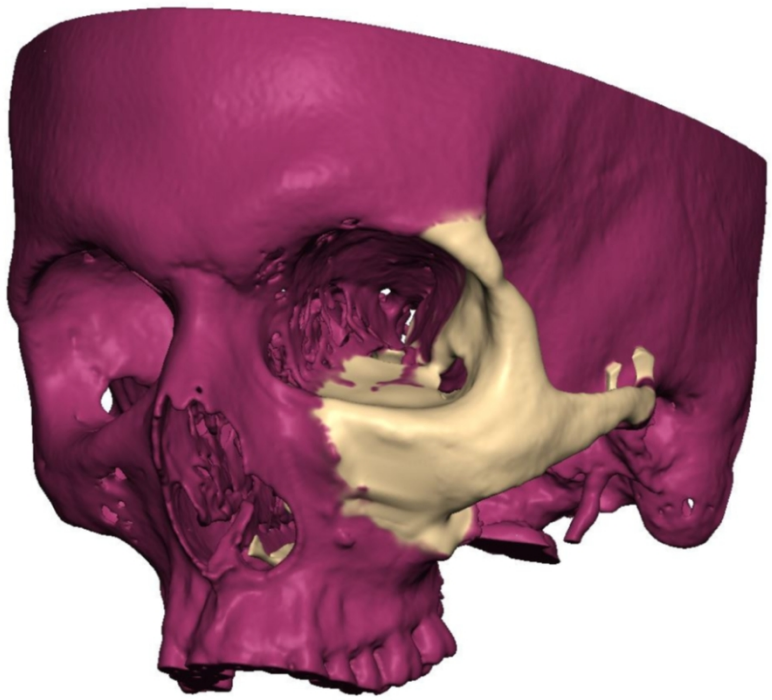

Figure 3. Designing of missing region using mirror-based reconstruction approach

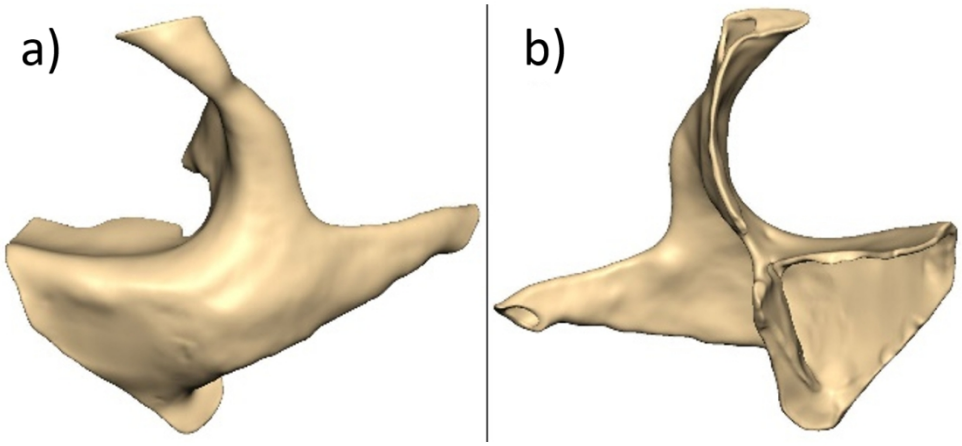

Figure 4. a) The outer (superficial) side of the hollow implant, and b) the inside (deep) side of the implant

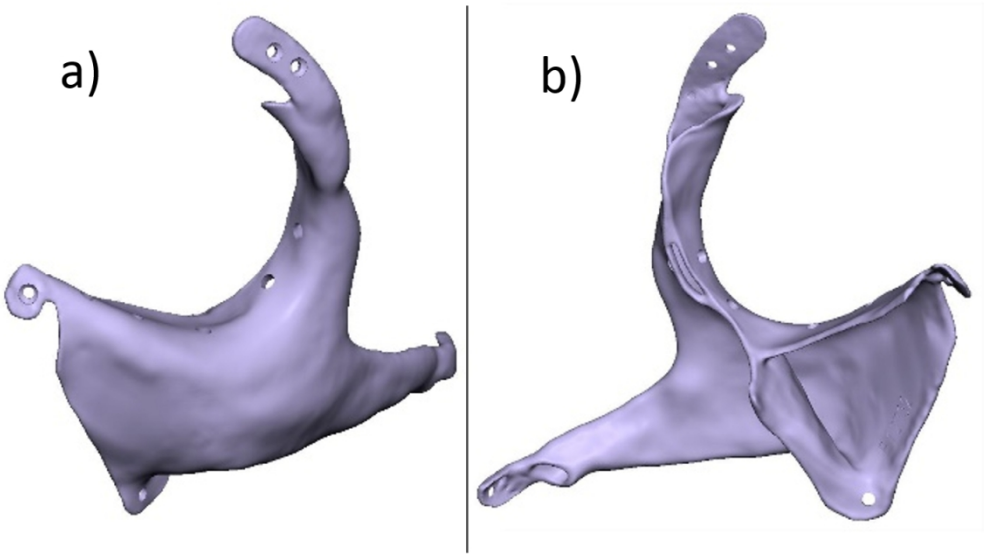

Figure 5. Completed implant design

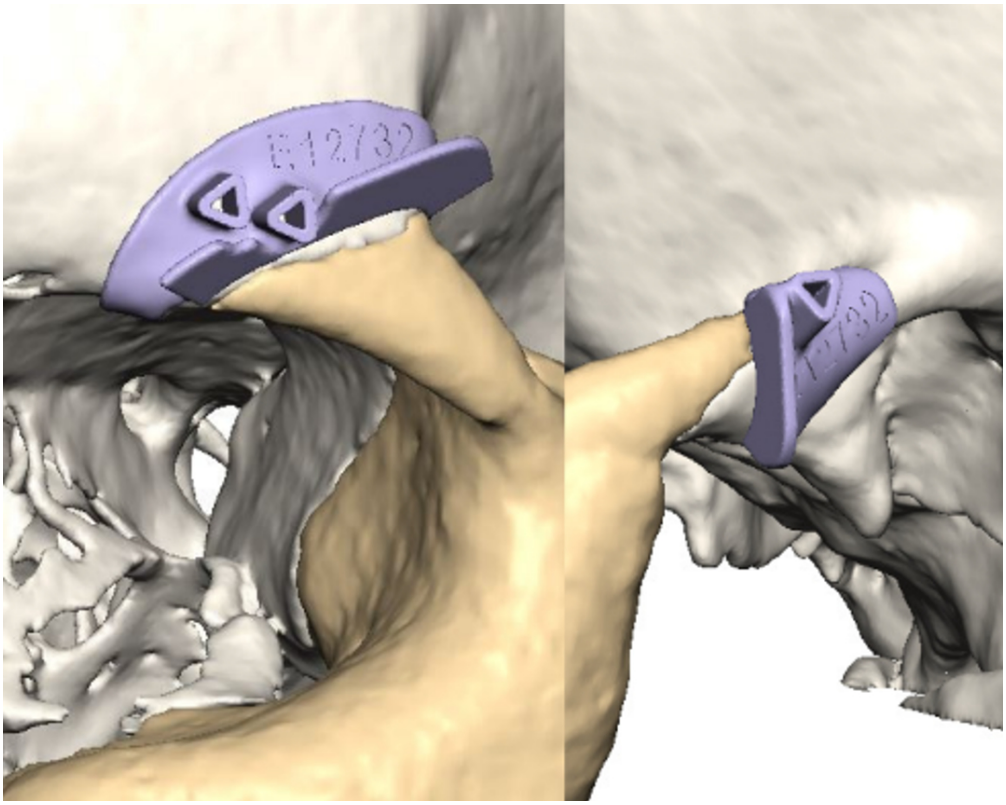

Figure 6. The surgical guides for disease removal

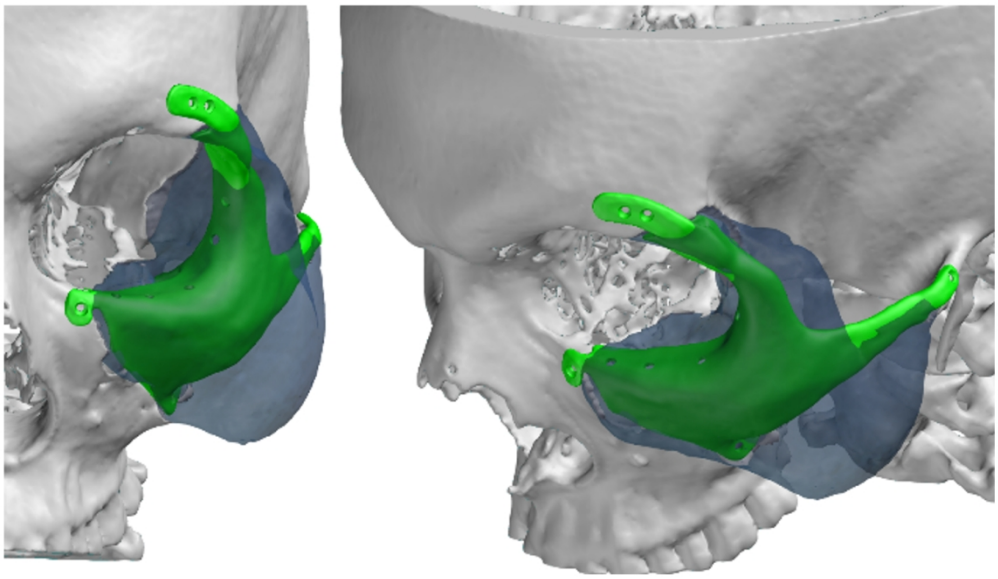

Figure 7. Analysis of the overlap of the modelled implant with the removed disease

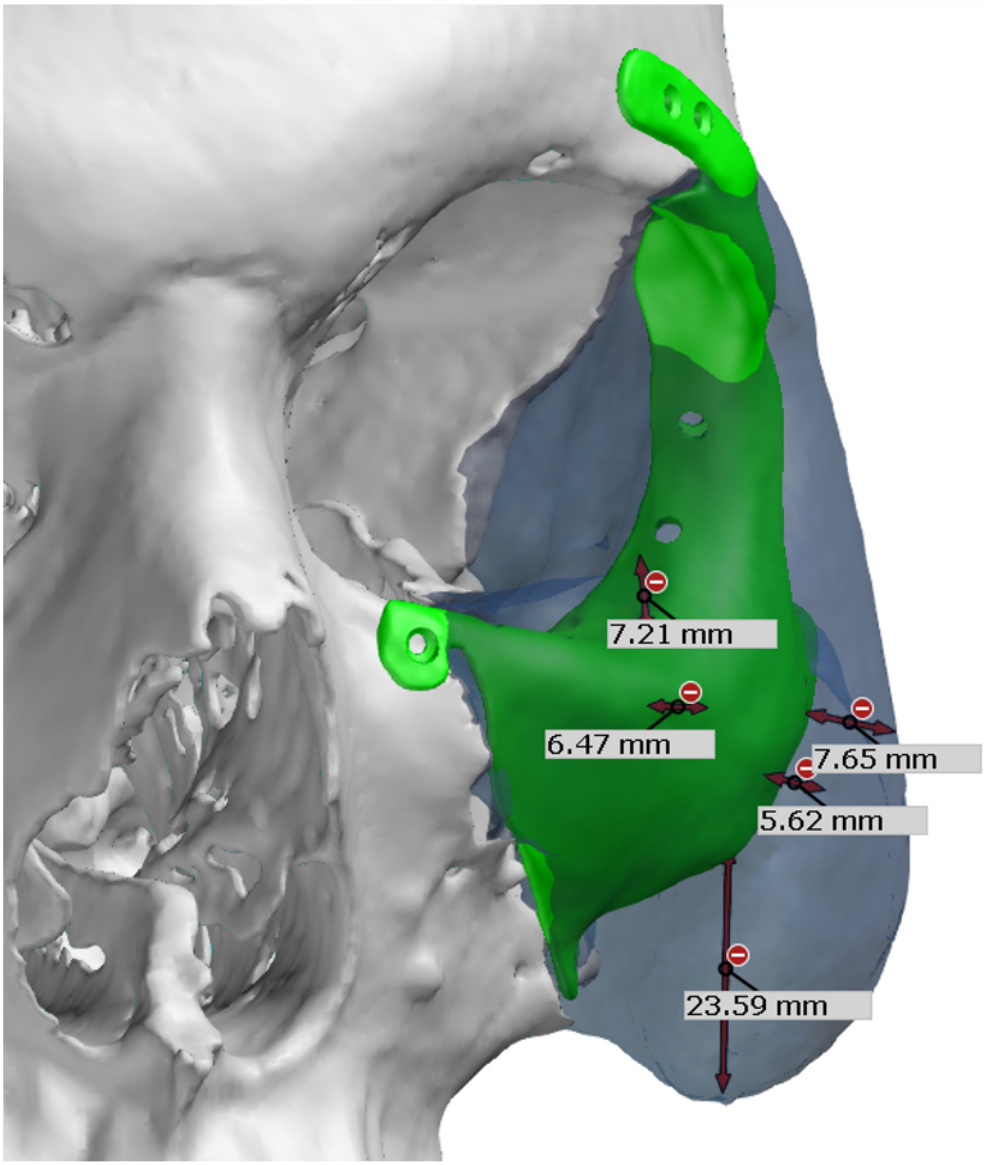

Figure 8. Distance between disease and implant at five control points

Figure 9. Implant fabricated from Titanium alloy

Figure 10. The guides with 1.25 mm openings which allow fixation during bone excision

Figure 11. Image a) and b) showing surgical procedure on the patient, and c) the condition after the procedure

Figure 12. Condition before and after the surgical procedure

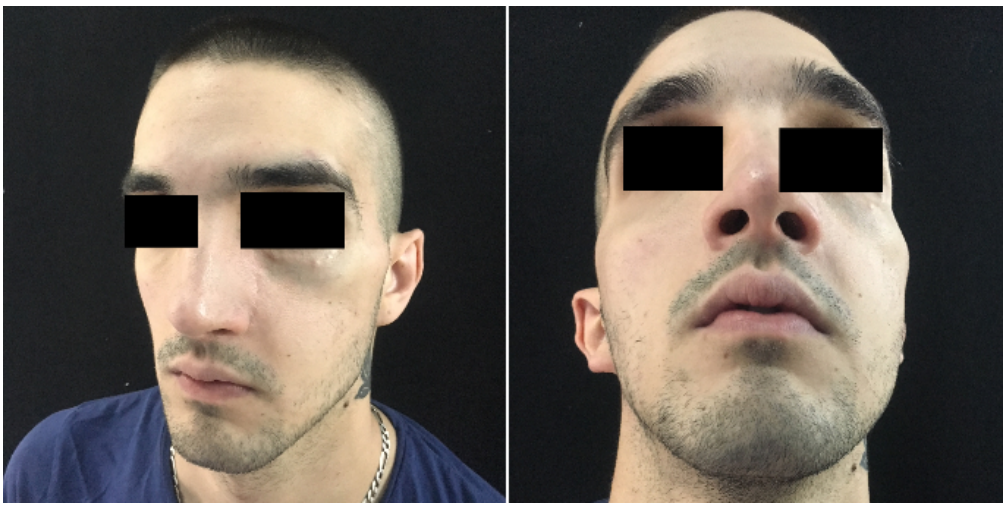

Figure 13. Post-operative check-up

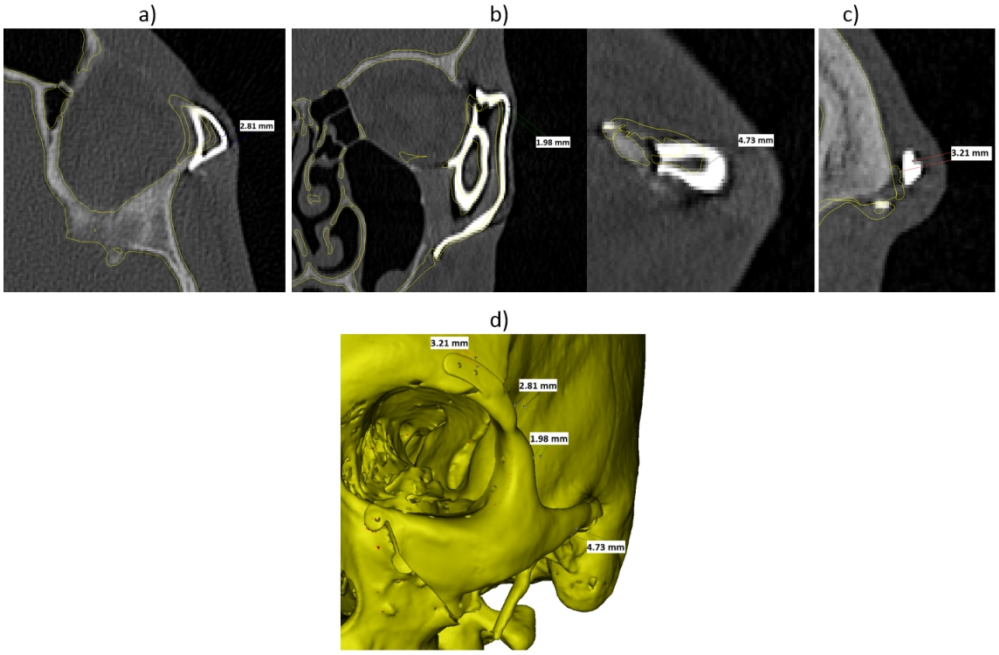

Figure 14. Post-operative scan with measurements on a) axial view, b) coronal view, c) sagittal view and d) the locations on where the measurements have been taken

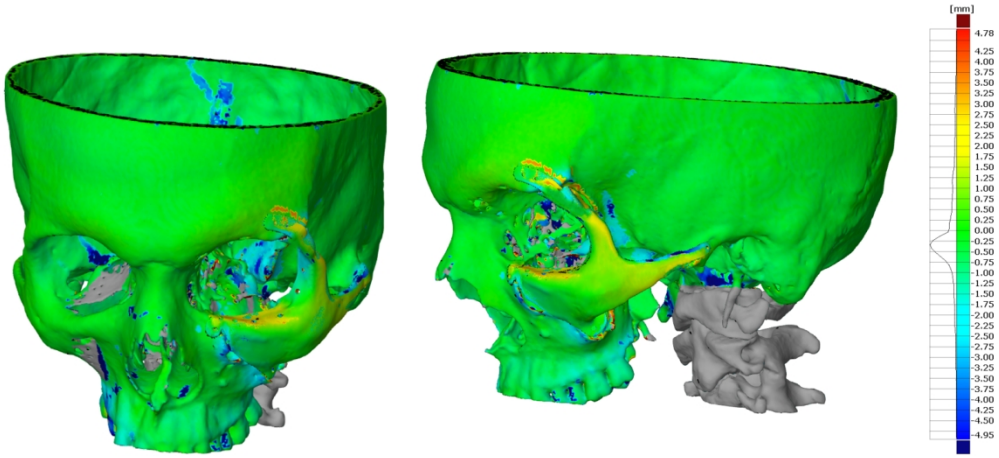

Figure 15. CAD-Inspection analysis of 3D models from pre-operative plan and the post-operative scan